Dynamic balancing of mechanisms with flexible links

Meijaard, J.P.; van der Wijk, V.

DOI
10.1016/j.mechmachtheory.2022.104784

Publication date
2022

Document Version
Final published version

Published in
Mechanism and Machine Theory

Mechanism and Machine Theory 172 (2022) 104784

Contents lists available at ScienceDirect

Mechanism and Machine Theory

journal homepage: www.elsevier.com/locate/mechmt

Research paper

Dynamic balancing of mechanisms with flexible links

J.P. Meijaard *, V. van der Wijk

Delft University of Technology, Faculty of Mechanical, Maritime and Materials Engineering, Department of Precision and Microsystems Engineering, Mekelweg 2, NL-2628 CD Delft, The Netherlands

ARTICLE INFO

Keywords:
Dynamic balance
Similarity
Flexible mechanisms
Modal balancing
Four-bar mechanism

ABSTRACT

The dynamic balancing of flexible mechanisms, that is, the reduction or elimination of shaking forces and shaking moments on the support structure, is considered. Two approaches are pursued: one uses similarity and the other modal balancing. A single rotating link can be balanced by a properly scaled countermass, for which balancing criteria are given. If all balancing conditions are satisfied, shaking force balance can even be achieved if geometric non-linearities are taken into account. This single link can be extended to a translator. Owing to the unscaled pitch of the translator and the asymmetric driving motor, no perfect shaking force balance is achieved, but the results can be considered satisfactory. Then, the dynamic balancing of a four-bar mechanism with a flexible coupler by means of modal balancing is shown. If the coupler is supported at the nodes of the first free vibration mode, this mode can be suppressed in the shaking force and shaking moment response. By supporting the coupler at four points with two whippletree mechanisms, the contribution of the first three symmetric vibration modes can be significantly reduced.

1. Introduction

The forces and moments a moving mechanism exerts on its foundation often have adverse effects and need to be reduced or eliminated. This can be done by dynamic balancing, that is, by making changes to the design, most often by redistributing the mass or by changing the structure of the mechanism. At the same time, a dynamically balanced mechanism is less sensitive to disturbances arising from the environment through the foundation, as the disturbing motion has less influence on the relative motions of its parts. Dynamic balancing of mechanisms consisting of rigid parts has been the subject of a large number of studies, such as [1–6], and several literature reviews are available [7–10]. The most common methods add counterweights and counterrotating rotors to a given mechanism, but also inherently balanced mechanisms are used. On the other hand, the influence of the flexibility of links or other parts of the mechanisms on the dynamic balance has received relatively little attention. The influence of deformation on the dynamic balance can become important for light-weight mechanisms operating at high speeds and for precision engineering applications. A field in which there has been a considerable interest in dynamically balancing systems with flexibility is rotordynamics. Modal balancing was introduced by Meldahl [11], Federn [12] and Bishop and Gladwell [13]; further literature can be found in review articles and textbooks [14–16]. The problems of rotordynamics are restricted, as the motion of rotors is quite special with mainly rotational motion, and their mass is nearly symmetrically distributed with respect to the axis of rotation.

Several studies deal with the influence that the flexibility and the adding of masses to balance a mechanism have on its dynamics and the shaking forces and shaking moments. Walker and Haines [17] found that in a completely shaking-force balanced six-bar mechanism, vibrations could counter the benefits of the additional balance masses. Xi and Sinatra [18] studied the influence of

* Corresponding author.
E-mail address: j.p.meijaard@tudelft.nl (J.P. Meijaard).

https://doi.org/10.1016/j.mechmachtheory.2022.104784
Received 30 November 2021; Received in revised form 1 February 2022; Accepted 14 February 2022
Available online 12 March 2022

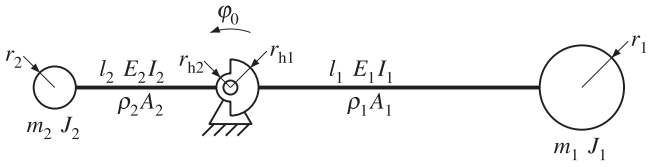

Fig. 1. Balanced compliant rotating arm.

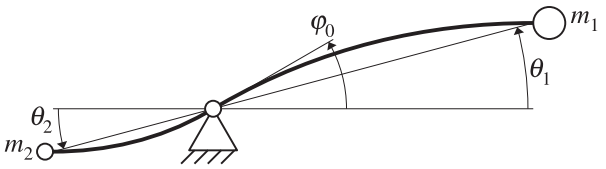

Fig. 2. Elementary model of a balanced compliant rotating arm in a deformed state.

adding balance masses on the vibrations of the links of a four-bar mechanism; they found that the amplitude of the vibrations could be increased by the additional mass. Yu and Lin [19,20] used the redundancy of the drives at the crank as well as at the rocker of a four-bar mechanism to reduce the shaking forces.

Cross [21] pointed out the importance of the first vibration mode of hand-held devices such as tennis racquets and bats: it seems that the point to hold the device that felt best is a node of the vibration mode rather than the centre of percussion calculated from rigid-body dynamics.

A first attempt to balance a flexible link was made by Kalas [22], who investigated a five-bar linkage, as in a parallel manipulator, with a flexible link. He modelled the flexible link by pseudorigid bodies [23], to which standard balancing techniques for rigid-link mechanisms were applied. Several lower-order eigenmodes in the response could be effectively suppressed.

Two approaches are taken in this article: firstly, the use of similarity and, secondly, the use of modal balancing. In the similarity approach, a mechanism is balanced by a scaled version of it. In modal balancing, the design is chosen in such a way that the linear vibration modes that are excited by the motion or the actuators do not give rise to resultant shaking forces or shaking moments. Frequently, this can only be achieved for a finite number of modes. The effectiveness is checked by the program Spacar, which can simulate the motion of multibody systems with flexible links [24].

Section 2 considers a single rotating arm, whereas in Section 3, two of these arms are applied in a translator. Section 4 considers the shaking force balancing of a beam and Section 5 applies the results to a four-bar mechanism with a flexible coupler. The article ends with conclusions. Preliminary studies have been presented in two conference contributions [25,26].

2. Similarity approach to balancing of a single rotating arm

An arm driven at a rotation point at its centre of mass is considered. The link consists of a hub rotating around a fixed axle and two flexible beams attached to it with rigid bodies connected to their ends, as shown in Fig. 1. In the simplest model, the beams and the hub are massless and the bodies are point masses. In a more detailed model, the beams have a uniformly distributed mass and the bodies have a finite size, as has the hub. The deflection due to gravity is neglected, which is allowed for most small devices. A controlled actuator drives the link at the hub with a prescribed angle.

2.1. Elementary lumped-mass model

In an elementary model, the dimensions of the hub and the bodies are neglected, as is the distributed mass of the beams. The beam to be balanced has a length l_1 and a flexural rigidity E_1I_1, where E_1 is Young's modulus of the material of the beam and I_1 is the second central area moment of the cross-section, and a point mass of m_1 is attached to the tip of the beam. This beam is balanced by a second beam of length l_2 and flexural rigidity E_2I_2, where E_2 and I_2 are the corresponding Young's modulus and second central area moment; the tip point mass is m_2. For the invariance of the position of the centre of mass, it is necessary to have

$$m_1 l_1 = m_2 l_2, \tag{1}$$

which puts the centre of mass of the system at the centre of the hub if the beams were rigid.

It is assumed that the deflections of the beams remain small, so linearized equations of motion can be used. Furthermore, the axial deformation of the beams is neglected. Hereafter, it will be discussed to what extent these assumptions can be relaxed. The rotation angle at the hub is denoted by φ_0, and the absolute angles of the lines joining the hub with the tip masses are denoted by θ_1 and θ_2, see Fig. 2. The equations of motion of the two point masses are

$$m_1 l_1^2 \ddot{\theta}_1 + \frac{3E_1I_1}{l_1}(\theta_1 - \varphi_0) = 0, \quad m_2 l_2^2 \ddot{\theta}_2 + \frac{3E_2I_2}{l_2}(\theta_2 - \varphi_0) = 0. \tag{2}$$

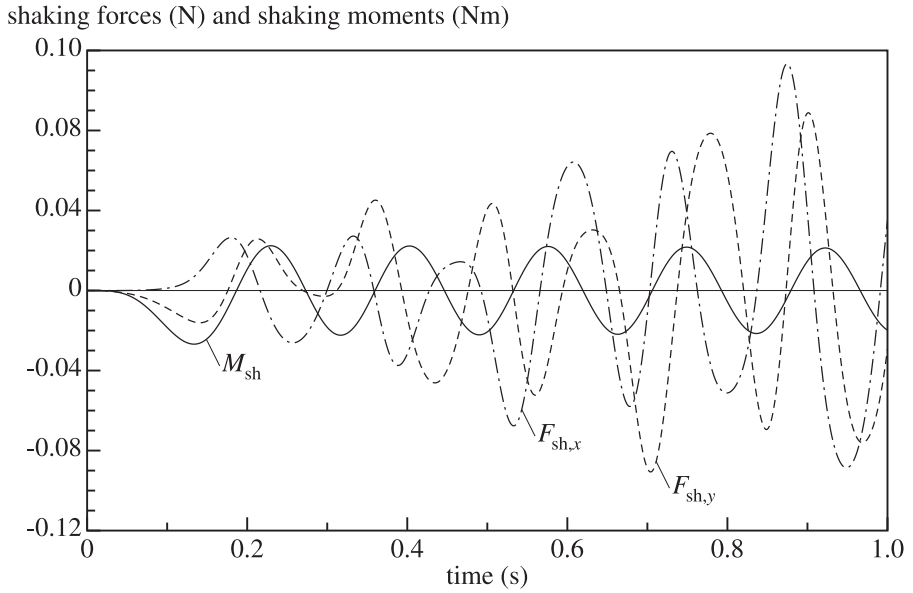

Fig. 3. Shaking forces in the horizontal direction, $F_{sh,x}$, (dashed–dotted) and the vertical direction, $F_{sh,y}$, (dashed) and the shaking moment, M_{sh}, (continuous) for a compliant rotating beam with tip masses.

The driving torque, M_0, follows from the balance of moments at the hub as

$$M_0 = \frac{3E_1I_1}{l_1}(\varphi_0 - \theta_1) + \frac{3E_2I_2}{l_2}(\varphi_0 - \theta_2) \tag{3}$$

and the lateral reaction force on the hub is

$$F_0 = \frac{3E_1I_1}{l_1^2}(\theta_1 - \varphi_0) - \frac{3E_2I_2}{l_2^2}(\theta_2 - \varphi_0). \tag{4}$$

The system is shaking force balanced if the position of the centre of mass does not change, that is,

$$m_1l_1\theta_1 = m_2l_2\theta_2. \tag{5}$$

This means that the differential equations (2) for $m_1l_1\theta_1$ and $m_2l_2\theta_2$ must have one and the same solution, or, because of the balance condition (1), $\theta_1 = \theta_2$; this leads to the condition

$$\frac{E_1I_1}{l_1^2} = \frac{E_2I_2}{l_2^2}\,. \tag{6}$$

The same result can be obtained from the condition that the lateral force in Eq. (4) must be zero. Because of the balance condition (1), Eq. (6) may be written as

$$E_1I_1m_1^2 = E_2I_2m_2^2\,. \tag{7}$$

It appears that the longer beam must be stiffer and the beam with a larger mass must be more flexible, contrary to what is generally chosen in designs. These conditions lead to equal eigenfrequencies of the two beams if the hub is held fixed, as follows from Eq. (2).

In the non-linear range of motion, the two point masses can still have similar motions, one scaled and rotated by 180 degrees with respect to the other, and the normal and tangential forces on the masses are the same. As the dimensionless force, E_iI_i/l_i^2 ($i = 1, 2$), proportional to the Euler buckling load, is also the same for both beams, this similar motion is possible and the link remains shaking force balanced for finite motions. If the axial deformation of the beam is not neglected, an additional condition is needed on the axial stiffness values E_1A_1 and E_2A_2 of the beams, with A_1 and A_2 the respective areas of their cross-sections, viz

$$E_1A_1 = E_2A_2. \tag{8}$$

Because the normal forces in both beams are the same, the extensions are proportional to the lengths of the beams and the configurations of the beams remain similar.

It is assumed that the motion of the link starts from a state of rest and no external disturbances are present. Different initial conditions or disturbances can lead to significant shaking forces; for instance, if the initial vibrations are in antiphase. For cyclic motions, the influence of the initial conditions fades away after some time if some damping is present.

As an example, the case is considered with $l_1 = 0.1$ m, $m_1 = 0.01$ kg, $E_1I_1 = 0.0045$ N m^2, $l_2 = 0.05$ m, $m_2 = 0.02$ kg, $E_2I_2 = 0.001125$ N m^2, and the mass per unit of length are $\rho_1A_1 = 0.024$ kg/m for the longer beam and $\rho_2A_2 = 0.0135$ kg/m

for the shorter beam, where ρ_1 and ρ_2 are the mass densities of the two materials of the beam; therefore, the mass of the longer beam is not negligible. The link is driven, starting from rest in a horizontal position, with a prescribed rotation angle given as a function of the time, t, by

$$\varphi_0 = \begin{cases} \Omega T_1[t^2/(2T_1^2) + 1/(4\pi^2)(\cos(2\pi t/T_1) - 1)] & (0 \le t \le T_1), \\ \Omega(t - T_1/2) & (t \ge T_1), \end{cases} \tag{9}$$

where the final angular velocity is chosen as $\Omega = 10$ rad/s and the acceleration time as $T_1 = 0.2$ s. For massless beams, the natural frequency of the two beams with tip mass is 5.85 Hz, but if the mass of the beams is taken into account, the first two frequencies become 5.69 Hz and 5.82 Hz. The system is modelled in the software system Spacar. Each beam is modelled with five planar beam elements, the spatial version of which is fully described in [27]. The motion is simulated over a period of 1 s, with the results for the shaking forces and shaking moment as shown in Fig. 3. Whereas a large shaking moment could be expected (moment balance was not considered), the shaking forces build up over time and reach values of the same order of magnitude as those for the unbalanced link (0.22 N). Therefore, the elementary lumped-mass model may not be accurate in practical cases and more refined balancing schemes are needed.

2.2. Extended model for a finite size of the hub and the bodies

Now, the finite size of the hub and the tip bodies are taken into account, but the mass of the beams and their axial strains are still neglected. In a linear model, the lateral force, F_i, and the moment, M_i, at the tip of a cantilever prismatic beam of length l_i and flexural rigidity E_iI_i can be related to the lateral tip displacement, v_i, and tip rotation, φ_i, by a stiffness matrix as

$$\begin{bmatrix} F_i \\ M_i \end{bmatrix} = \frac{E_iI_i}{l_i^3} \begin{bmatrix} 12 & -6l_i \\ -6l_i & 4l_i^2 \end{bmatrix} \begin{bmatrix} v_i \\ \varphi_i \end{bmatrix}. \tag{10}$$

If the hub with radius $r_{\mathrm{h}i}$ and the radius of the mass r_i are taken into account, the stiffness matrix with respect to the centre of the tip mass becomes

$$\frac{E_iI_i}{l_i^3} \begin{bmatrix} 12 & -6l_i - 12r_i \\ -6l_i - 12r_i & 4l_i^2 + 12l_ir_i + 12r_i^2 \end{bmatrix} \tag{11}$$

and the forcing term due to the rotation of the hub is given by

$$\frac{E_iI_i\varphi_0}{l_i^3} \begin{bmatrix} 6l_i + 12r_{\mathrm{h}i} \\ -2l_i^2 - 6l_ir_i - 12r_ir_{\mathrm{h}i} - 6l_ir_{\mathrm{h}i} \end{bmatrix}. \tag{12}$$

The equations of motion are therefore

$$\begin{aligned} &m_i\ddot{v}_i + \frac{E_iI_i}{l_i^3}\left[12v_i - (6l_i + 12r_i)\varphi_i - (6l_i + 12r_{\mathrm{h}i})\varphi_0\right] = 0, \\ &J_i\ddot{\varphi}_i + \frac{E_iI_i}{l_i^3}\left[-(6l_i + 12r_i)v_i + (4l_i^2 + 12l_ir_i + 12r_i^2)\varphi_i\right. \\ &\qquad \left. +(2l_i^2 + 6l_ir_i + 12r_ir_{\mathrm{h}i} + 6l_ir_{\mathrm{h}i})\varphi_0\right] = 0. \end{aligned} \tag{13}$$

From this it appears that the two beams have similar solutions if their geometric dimensions are similar, that is, all lengths of the second beam must be some scale factor, say f, as large as the corresponding lengths of the first beam. To ensure force balance, the mass must be scaled by the reciprocal of this scale factor, $1/f$. The flexural rigidities, however, must be scaled with f^2, as in Eq. (6). As the mass moments of inertia have the dimension of mass times length squared, these must scale as f. Corresponding angles are the same for both beams.

2.3. Further extension for beams with distributed mass

Subsequently, the distributed mass of the beams is taken into account. For small displacements, the differential equation for the lateral displacement is [28]

$$\rho_iA_i\ddot{v}_i + E_iI_iv_i'''' = 0, \tag{14}$$

where a prime denotes a derivative with respect to the coordinate s_i measured along the axis of the beam from the hub. The boundary conditions are

$$\begin{aligned} &s_i = 0: \quad v_i = r_{\mathrm{h}i}\varphi_0, \quad v_i' = \varphi_0; \\ &s_i = l_i: \quad E_iI_iv_i''' = m_i\ddot{v}_i + m_ir_i\ddot{v}_i', \quad E_iI_iv_i'' = -m_ir_i\ddot{v}_i - (J_i + m_ir_i^2)\ddot{v}_i'. \end{aligned} \tag{15}$$

With the time scale $\sqrt{\rho_iA_il_i^4/(E_iI_i)}$, the length scale l_i and the mass scale $\rho_iA_il_i$, the equation and the boundary conditions can be made dimensionless by the introduction of the dimensionless parameter combinations

$$\frac{m_i}{\rho_iA_il_i}, \quad \frac{J_i}{\rho_iA_il_i^3}, \quad \frac{r_i}{l_i}, \quad \frac{r_{\mathrm{h}i}}{l_i}. \tag{16}$$

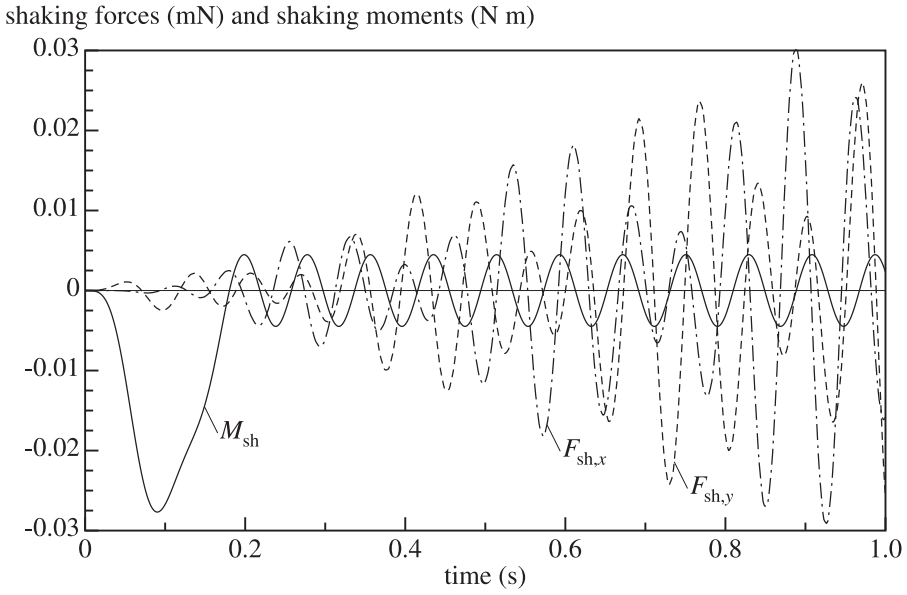

Fig. 4. Shaking forces in the horizontal direction, $F_{sh,x}$, (dash-dotted) and the vertical direction, $F_{sh,y}$, (dashed) and the shaking moment, M_{sh}, (continuous) for a compliant rotating beam with tip bodies.

If these four parameters are the same for both similar parts, similar solutions can exist for a fixed hub. If φ_0 has the same time evolution for both parts, also the dimensionless time has to be the same, which leads to similar solutions which scale with the length l_i. As the lateral force of the beams on the hub is given by $E_i I_i v_i'''(0)$, which scales as $E_i I_i / l_i^2$, we have as the outcome the balance conditions that the two parts are geometrically similar and the condition (6). Then, from the condition of equal time scales, it follows that

$$\rho_1 A_1 l_1^2 = \rho_2 A_2 l_2^2. \tag{17}$$

From the first dimensionless group of (16), the condition (1) now follows. Also the eigenfrequencies for the two parts for a fixed hub are now the same. A combination of the conditions (8) and (17) yields

$$\frac{E_1}{\rho_1 l_1^2} = \frac{E_2}{\rho_2 l_2^2}, \quad \text{or} \quad \frac{c_1}{l_1} = \frac{c_2}{l_2}, \tag{18}$$

where $c_1 = \sqrt{E_1/\rho_1}$ and $c_2 = \sqrt{E_2/\rho_2}$ are the speeds of sound for longitudinal waves in the two beams. This condition was derived by Nijdam [29]. The conditions for shaking force balancing a rotating flexible arm as in Fig. 1 with geometrically similar parts are therefore (1), (6), and two of the conditions (8), (17) and (18).

2.4. The general case of similarity balancing with two structures

For a general case, two structures of different size behave similarly with the same time scale if the speed of sound is proportional to the length scale, that is, the materials have the same Poisson ratio and $\sqrt{E/\rho}$ scales with f. As the mass must scale as $1/f$ for dynamic balance, and hence the mass per unit of area as $1/f^3$, this normally means that the out-of-plane width scales as $1/f^3$ if the material is the same, or the density scales with $1/f^3$ if the width is the same. For constant density, Young's modulus E has to scale as f^2 and for constant width, E has to scale as $1/f$. The first option could be realized if the smaller structure had some mass that does not contribute to the stiffness, for instance due to slits in the transverse direction, whereas the latter is difficult to realize. The use of metamaterials might be a solution, as density and stiffness need not scale in the same way for these materials. In particular, it is possible to reduce E more than ρ by a pattern of holes and so to reduce the speed of sound.

A compromise for structures composed of beams and concentrated masses can be made if similarity for the axial stiffness of the beams is not enforced and similarity for the mass moment of inertia of the cross-section of the beams is not imposed. In that case, identical materials can be used, the in-plane thickness of the beams scales as f^2 and the out-of-plane width scales as $1/f^4$. The eigenfrequencies scale with $\sqrt{EI/(\rho A l^4)}$, which remains the same. For the rigid parts, the width has to scale as $1/f^3$.

As an example, the case is considered with $E = 2.0 \times 10^{11}$ N/m^2, a Poisson ratio $\nu = 0.29$, $\rho = 8000$ kg/m^3, $l_1 = 0.1$ m and $l_2 = 0.05$ m, so $f = 0.5$, $m_1 = 0.01$ kg, $m_2 = 0.02$ kg, thicknesses $t_1 = 1$ mm and $t_2 = 0.25$ mm, widths $w_1 = 2$ mm, $w_2 = 32$ mm, radii of the hub of $r_{h1} = 10$ mm, $r_{h2} = 5$ mm, and radii of the tip masses $r_1 = 15$ mm and $r_2 = 7.5$ mm. The hub has a mass of $m_h = 0.001$ kg and the shear factor of the beams is 0.84. Moments of inertia of the concentrated masses are calculated on the assumption that they have the shape of uniform discs. The motion profile of the hub actuator is the same as in the previous example given by Eq. (9),

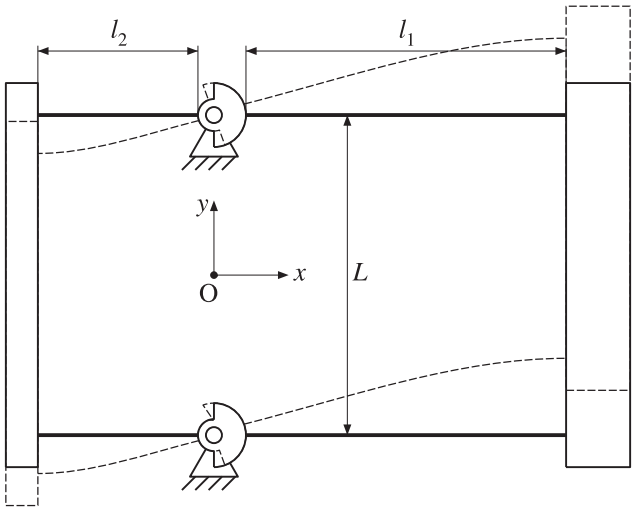

Fig. 5. Parallel-motion translator balanced by another translator; a deformed configuration is shown in dashed lines.

with $\Omega = 10$ rad/s and $T_1 = 0.2$ s. If the axial deformation of the beams, the shear deformation and the mass moment of inertia of the cross-sections of the beams are neglected, the shaking forces from the simulation are exactly equal to zero. If these simplifications are not made, the simulation gives the results shown in Fig. 4 and the first eigenfrequencies of the two parts differ by 0.002%. Note that the scale of the shaking forces is in mN, so these forces remain small.

3. Balanced translator

Next, the translator on the right side of the mechanism shown in Fig. 5 that is balanced by a scaled translator on the other side is considered. The mechanism is composed of the flexible rotating links of Fig. 1 connected by rigid blocks that are intended to translate. The scaling is only done in one direction, as the pitch L between the links is the same at both translators, so near-perfect shaking force balance may not be expected in all cases. The beams can still rotate at their hubs, but they are rigidly fixed to the translators. The mechanism can be driven at one of the hubs, or at both hubs to have a more symmetric forcing. Translators are used, amongst others, in optical systems for focusing lenses and operating shutters and for slicing samples.

The same balancing principles as for the single rotator are used. As an example, the same beams and hubs as in the previous example of the rotator are taken, but there are now two sets and the end masses are replaced by rigid rectangular blocks with in-plane lengths of 0.12 m and breadths of 20 mm and 10 mm, and out-of-plane widths of 10 mm and 40 mm respectively, made of a polymer with mass density 900 kg/m^3, so the masses of the blocks are $m_1 = 0.0216$ kg and $m_2 = 0.0432$ kg. The two beams are a pitch $L = 0.1$ m apart. Effects of shear, axial elongation and moment of inertia of the beams are taken into account. The hub is driven by a prescribed moment given by

$$M = \begin{cases} M_0[t/T_1 - \sin(2\pi t/T_1)/(2\pi)] & (0 \le t \le T_1), \\ M_0 & (t \ge T_1), \end{cases} \tag{19}$$

where the final value of the moment is chosen as $M_0 = 0.05$ N m if only the lower hub is driven or as $M_0 = 0.025$ N m if both hubs are driven and the rise time is $T_1 = 0.02$ s. In both cases, the translator vibrates between a minimum displacement of about zero and a maximum displacement of about 6 mm.

Fig. 6 shows the resulting shaking forces and shaking moment with respect to the origin O at the centre of the mechanism in the case of asymmetric forcing. The shaking moment is not balanced, as this was not a part of the design. The normal forces in the beams do not scale in the right way, which is due to the imperfect similarity. Nevertheless, it is seen that the shaking forces are quite small, so there is a reasonable dynamic force balance. Indeed, the shaking forces are reduced by a factor of 100 with respect to the unbalanced mechanism for the same motion amplitude. The shaking force results mainly from the vibration in the second eigenmode.

Fig. 7 shows the results for the case of symmetric forcing, where both hubs are actuated. Although the shaking moment is about the same as for the asymmetric forcing, the resulting shaking forces are smaller by a factor of 15. Note that there is no damping in the system, so the vibrations continue to exist over time. Ultimately, a large energy transfer between modes can occur. Adding some damping will prevent this.

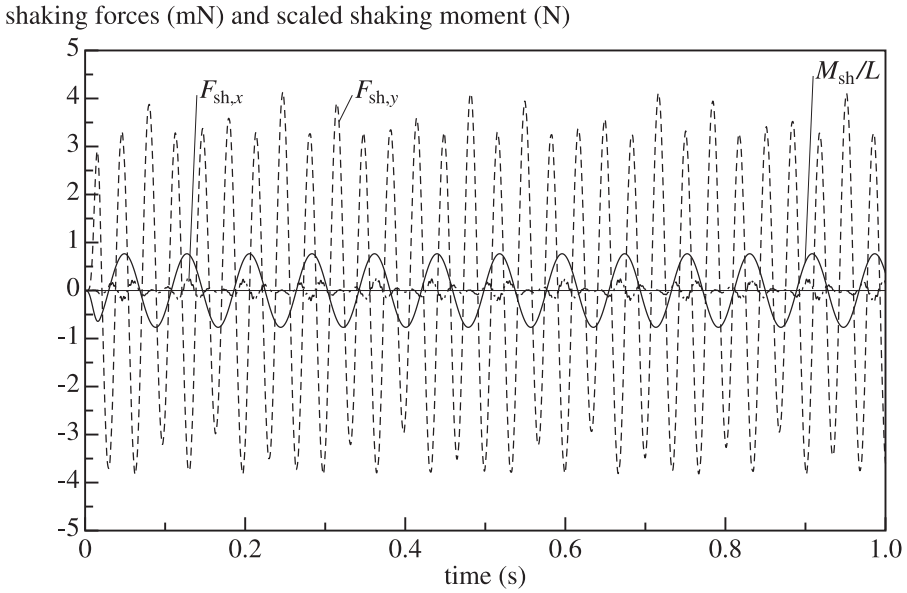

Fig. 6. Shaking forces in the horizontal direction, $F_{sh,x}$, (dash-dotted) and the vertical direction, $F_{sh,y}$, (dashed) and the scaled shaking moment with respect to the centre of the mechanism between the two hubs, M_{sh}/L, (continuous) for the translator with asymmetric forcing.

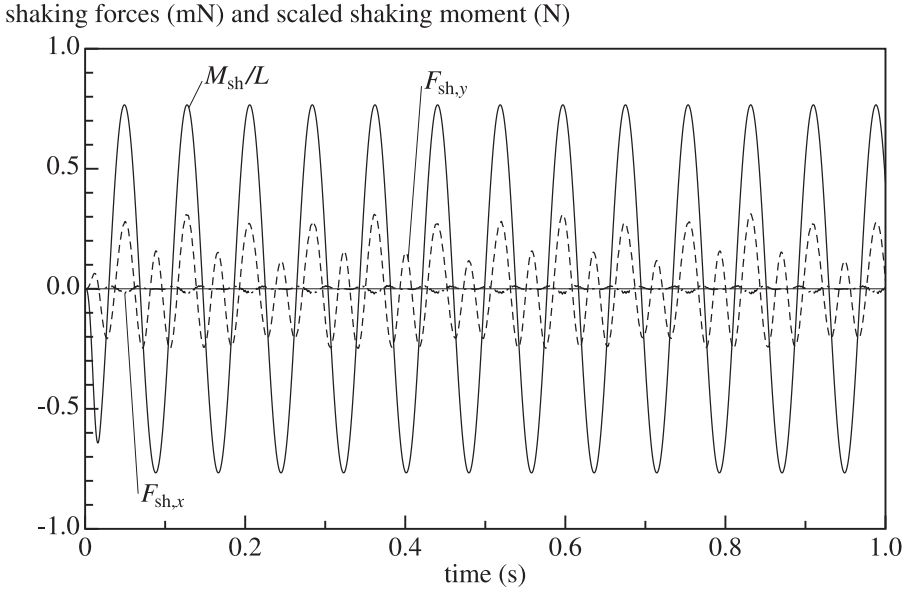

Fig. 7. Shaking forces in the horizontal direction, $F_{sh,x}$, (dash-dotted) and the vertical direction, $F_{sh,y}$, (dashed) and the scaled shaking moment with respect to the centre of the mechanism between the two hubs, M_{sh}/L, (continuous) for the translators with symmetric forcing.

4. Supporting a flexible beam for dynamic balance

The central question is how a flexible beam can be supported in such a way that the vibrations of the beam yield small shaking forces and shaking moments. As axial and torsional vibrations normally have higher natural frequencies, and the excitation of the mechanism is mostly concentrated at low frequencies, only the influence of lateral vibrations will be considered. Furthermore, the beam moves in a plane and no out-of-plane vibrations are taken into account.

It is assumed that the beam is supported at a number of discrete points and the displacements in these points are summed with some weights to get the displacement of the point or points with which the beam is connected to the other links or the ground. The precise way this can be done has to be decided in the design of a mechanism. The optimal choice of the support points and the weights can be made on the basis of several criteria. As in the case of balancing of flexible rotors, modal balancing can be used, in

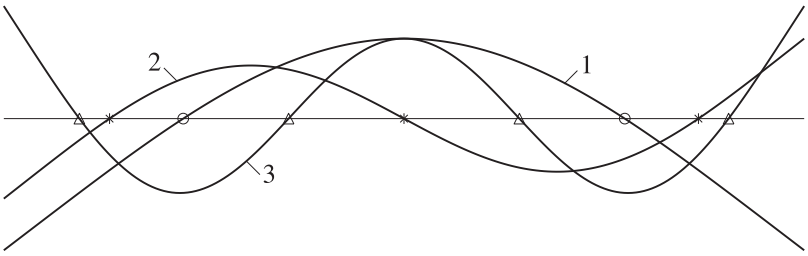

Fig. 8. First three vibration modes of a free beam with nodes indicated by markers.

which a number of vibration modes are dynamically balanced. An alternative criterion is the minimization of the deflection of the beam under a uniform load, so the displacement of the centre of mass of the beam due to the deformation is as small as possible. Preference is given to modal balancing, because it avoids resonances in the balanced modes. The condition of shaking moment balance for the rigid-body motion gives some additional constraints if the balancing needs to be possible with counterrotating counterweights [30].

With one support point to choose, the obvious choice is the point of the centre of mass. With two support points, the points can be chosen as the two nodes of the first vibration mode of the beam as a free body. Because these points remain fixed if the beam vibrates in its first mode, no forces are transmitted if these nodes are fixed. The vibration frequencies and modes can be found in several places, for instance in the book by den Hartog [28]. The frequencies are found by solving the characteristic equation, which reads

$$\cos\lambda\cosh\lambda - 1 = 0, \quad \lambda = l\sqrt[4]{\frac{\rho A\omega^2}{EI}}, \tag{20}$$

for a beam of uniform cross-section of length l, flexural rigidity EI and mass per unit of length ρA, where ω is the natural circular frequency. This equation can be rewritten as

$$\left(\cos\frac{\lambda}{2}\sinh\frac{\lambda}{2} + \sin\frac{\lambda}{2}\cosh\frac{\lambda}{2}\right)\left(\cos\frac{\lambda}{2}\sinh\frac{\lambda}{2} - \sin\frac{\lambda}{2}\cosh\frac{\lambda}{2}\right) = 0. \tag{21}$$

This shows that there is a root of multiplicity four at $\lambda = 0$, to which correspond two rigid-body modes. Putting the first expression between brackets equal to zero yields the symmetric vibrations modes, which can be written as

$$\cosh\frac{\lambda}{2}\cos\lambda\xi + \cos\frac{\lambda}{2}\cosh\lambda\xi, \tag{22}$$

where ξ, $-1/2 \le \xi \le 1/2$, is the dimensionless coordinate along the axis of the beam measured from the centre. Equating the second expression between brackets in Eq. (21) to zero yields the antisymmetric vibration modes,

$$\sinh\frac{\lambda}{2}\sin\lambda\xi + \sin\frac{\lambda}{2}\sinh\lambda\xi. \tag{23}$$

The first three vibration modes are shown in Fig. 8 and the eigenfrequencies and zeros for the first few eigenmodes are given in Table 1. They are given in a dimensionless form, that is, as $\omega = \lambda^2$, and the dimensionless coordinate ξ. For higher-order modes, the frequencies can be approximated by $\lambda_k^2 = (k+1/2)^2\pi^2$ and the zeros by $\pm(2i-1)/(2k+1)$ $(i = 1,\dots,(k+1)/2)$ for the symmetric modes and by $\pm 2i/(2k+1)$ $(i = 0,\dots,k/2)$ for the antisymmetric modes. So for the balancing of the first vibration mode, it is sufficient to support the beam at $\pm 0.275842477\,l$ from the centre.

Another way to balance the beam would be to require that the centre of mass of the beam is displaced as little as possible by a static uniform lateral load on the beam, as for gravity loading or a uniform acceleration. If the supports are symmetrically located at $\xi = \pm\xi_0$, the deflection becomes, for a uniform load EI/l^3,

$$\begin{aligned}
\frac{v}{l} &= -\frac{1}{16}\xi_0^2 + \frac{1}{4}\xi_0^3 - \frac{1}{24}\xi_0^4 + \left(\frac{1}{16} - \frac{1}{4}\xi_0\right)\xi^2 + \frac{1}{24}\xi^4 && (-\xi_0 \le \xi \le \xi_0),\\
\frac{v}{l} &= -\frac{1}{16}\xi_0^2 + \frac{1}{3}\xi_0^3 - \frac{1}{24}\xi_0^4 - \frac{1}{4}\xi_0^2|\xi| + \frac{1}{16}\xi^2 - \frac{1}{12}|\xi|^3 + \frac{1}{24}\xi^4 && (\xi_0 \le |\xi| \le \tfrac{1}{2}).
\end{aligned} \tag{24}$$

The displacement of the centre of mass can be found by integrating the expression of the deflection v/l over the length of the beam and dividing by the length. The result is

$$\frac{v_0}{l} = 2\int_0^{1/2}\frac{v}{l}\mathrm{d}\xi = \frac{1}{320} - \frac{1}{8}\xi_0^2 + \frac{1}{3}\xi_0^3 - \frac{1}{12}\xi_0^4. \tag{25}$$

This deflection is minimal if $\xi_0 = (1/2)(3-\sqrt{6}) \approx 0.275255129$, for which value the deflection attains its minimum, equal to zero, at $\xi = \pm\xi_0$. Note that this point is very close to the position of the node of the first vibration mode, about 0.1% of the beam length away from it. As the results are so close, we will concentrate on modal balancing.

In some cases, it can be advantageous to support the beam at symmetrically located reciprocal points, that is, at a distance equal to the radius of gyration away from the centre. Then lateral forces applied at one support point do not give rise to motion, or reaction forces, at the other support point. For a uniform beam, the radius of gyration is $l\sqrt{3}/6 \approx 0.288675135\,l$.

Table 1
Dimensionless eigenfrequencies and zeros of the eigenmodes for the vibration modes of a free beam.

Mode k	Frequency ω_k	Zeros $\xi_{k,i}$	
1	22.373285448061	±0.275842477297642	
2	61.672822867920	0	±0.367892044836738
3	120.903391727124	±0.144196546027406	±0.405557156878000
4	199.859448127201	0	±0.223219952829764
		±0.426547236535226	
5	298.555535298176	±0.090872761949790	±0.273545148582375
		±0.439902184294380	
6	416.990785835445	0	±0.153816743433199
		±0.308384299946894	±0.449148005799258
7	555.165247566790	±0.066667818619707	±0.199974461177663
		±0.333933062067607	±0.455928271552871
8	713.078917978436	0	±0.117648031330238
		±0.235271585291052	±0.353470348802706
		±0.461113180787307	
9	890.731797198328	±0.052631539648058	±0.157895608677945
		±0.263137734134352	±0.368894522616056
		±0.465206530177909	
10	1088.123885220101	0	±0.095238061218115
		±0.190476979213647	±0.285696045172047
		±0.381380758557262	±0.468520193970497
11	1305.255182044067	±0.043478262272491	±0.130434751486348
		±0.217392024502036	±0.304331171678712
		±0.391695475204462	±0.471257568407845
12	1542.125687670212	0	±0.080000001234916
		±0.159999971369851	±0.240000662541769
		±0.319984677944420	±0.400359837188104
		±0.473556962935217	

For the case that also higher-order modes need to be considered in the dynamic balance, a more general approach is proposed. It is assumed that the beam is supported in a number of points and a weighted sum of the displacements at these points is taken as an approximation of the displacement of the centre of mass of the vibrating beam. This is to say, there are n connection points at the positions ξ_i, with lateral displacements $v_i = v(\xi_i)$, $(i = 1, \ldots, n)$, and the weights are W_i. The resulting approximation of the displacement, v_0, of the centre of mass is

$$v_0 = \sum_{i=1}^{n} W_i v_i. \tag{26}$$

A translation of the beam as a rigid body should result in the same displacement of the centre of mass, which leads to the condition

$$\sum_{i=1}^{n} W_i = 1\,. \tag{27}$$

In addition, a rotation as a rigid body about the centre of mass does not give a displacement of the centre of mass, so a second condition is

$$\sum_{i=1}^{n} W_i \xi_i = 0. \tag{28}$$

This condition is automatically satisfied if the connection points and the weights are chosen to be symmetric with respect to the centre of the beam. With a symmetric distribution of the support points and the corresponding weights, the antisymmetric vibration modes are automatically force balanced. For an odd number of support points, the central point is always a support point, whereas for an even number of support points, these can be split into two symmetrical groups. This means that the case with an odd number of support points is better suited for beams that have a rotation about their central point as their main motion, whereas the case with an even number of support points is better suited for beams used as links in mechanisms.

For the case with three support points, $\xi_2 = 0$, $\xi_1 = -\xi_3$ and $W_3 = W_1$; furthermore, as $W_1 + W_2 + W_3 = 1$, $W_1 = W_3 = (1 - W_2)/2$. To balance the first and the second symmetric vibration modes, the conditions

$$W_2\psi_1(0) + (1 - W_2)\psi_1(\xi_3) = 0, \quad W_2\psi_3(0) + (1 - W_2)\psi_3(\xi_3) = 0 \tag{29}$$

must be satisfied. Here, the vibration modes are denoted by ψ_1 and ψ_3, which are given by Eq. (22). Apparently,

$$\frac{\psi_1(\xi_3)}{\psi_1(0)} = \frac{\psi_3(\xi_3)}{\psi_3(0)} = \frac{-W_2}{1 - W_2} \tag{30}$$

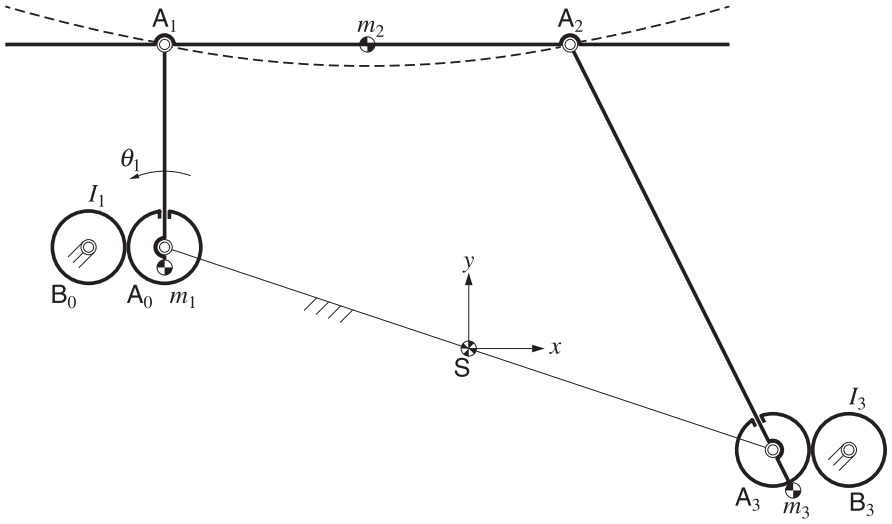

Fig. 9. Partially shaking force and shaking moment balanced four-bar mechanism with a flexible coupler, countermasses and counterrotating wheels; a deformed shape of the coupler is shown as a dashed line.

is needed, so if the modes are normalized to have a value equal to one at the centre of the beam, the distance ξ_3 is the place where the two modes intersect, that is, $\psi_1(\xi_3) = \psi_3(\xi_3)$. This is the case at the point $\xi_3 = 0$ by definition and at $\xi_3 = 0.356629311$, where $\psi_1(\xi_3) = \psi_3(\xi_3) = -0.561604905$. The weight W_2 is found from $W_2 = -\psi_1(\xi_3)/(1 - \psi_1(\xi_3))$. The results can be summarized as

$$\begin{aligned} \xi_1 &= -0.356629311, \quad W_1 = 0.320183421, \\ \xi_2 &= \ \ 0, \qquad\qquad W_2 = 0.359633159, \\ \xi_3 &= \ \ 0.356629311, \quad W_3 = 0.320183421. \end{aligned} \tag{31}$$

Now, the case with four support points is considered. The points are located symmetrically with respect to the centre of the beam. The weights are also symmetric and are given by W_1, $W_2 = 1/2 - W_1$, $W_3 = W_2$ and $W_4 = W_1$, and the coordinates are $\xi_1 = -\xi_4$, $\xi_2 = -\xi_3$, ξ_3 and ξ_4, so the three parameters W_1, ξ_3 and ξ_4 still need to be determined. These are chosen to make the first three symmetric vibration modes balanced. This means that the conditions

$$2W_1\psi_i(\xi_4) + (1 - 2W_1)\psi_i(\xi_3) = 0, \quad (i = 1, 3, 5) \tag{32}$$

must be fulfilled. Apparently,

$$\frac{\psi_i(\xi_3)}{\psi_i(\xi_4)} = \frac{-2W_1}{1 - 2W_1}, \quad (i = 1, 3, 5) \tag{33}$$

so the ratios of the amplitudes at the two support points on either side of the centre must be the same for all three vibration modes. The appropriate values of the two distances ξ_3 and ξ_4 can be numerically determined and the weight W_1 can be obtained from $W_1 = -\psi_1(\xi_3)/[2\psi_1(\xi_4) - 2\psi_1(\xi_3)]$. The results can be summarized as

$$\begin{aligned} \xi_1 &= -0.394718293, \quad W_1 = 0.235140064, \\ \xi_2 &= -0.132607152, \quad W_2 = 0.264859936, \\ \xi_3 &= \ \ 0.132607152, \quad W_3 = 0.264859936, \\ \xi_4 &= \ \ 0.394718293, \quad W_4 = 0.235140064. \end{aligned} \tag{34}$$

5. Dynamic balancing of a planar four-bar mechanism with a flexible coupler

The beam considered in the previous section is used as a coupler in a planar four-bar mechanism as shown in Fig. 9. The lengths of the links are made dimensionless with the kinematic length of the coupler between the points A_1 and A_2, which has a unit length: the length of the crank is 0.5, the length of the rocker is $0.5\sqrt{5}$ and the length of the ground link is $0.5\sqrt{10}$. These lengths just satisfy the Grashof condition, so the crank can turn indefinitely with angle θ_1. In the initial position, the crank is perpendicular to the coupler, as shown in Fig. 9. The coupler is extended beyond its two joints to have a freedom in the relative positions of the joints. The mass is made dimensionless, so the coupler has a unit mass per unit of length and time is made dimensionless in such a way that the flexural rigidity is unity, whereas the other links are rigid and massless, except for the balance masses m_1 and m_3 placed at one tenth of the lengths of the crank and the rocker, so $m_1 = m_3 = 5m_2$, where m_2 is the total mass of the coupler. In order to obtain a partial moment balance of the mechanism, two counterrotating wheels are introduced with moments of inertia $I_1 = 0.1375m_2$ and $I_3 = 0.6875m_2$. These values of the balance masses and moments of inertia give a perfect force and moment

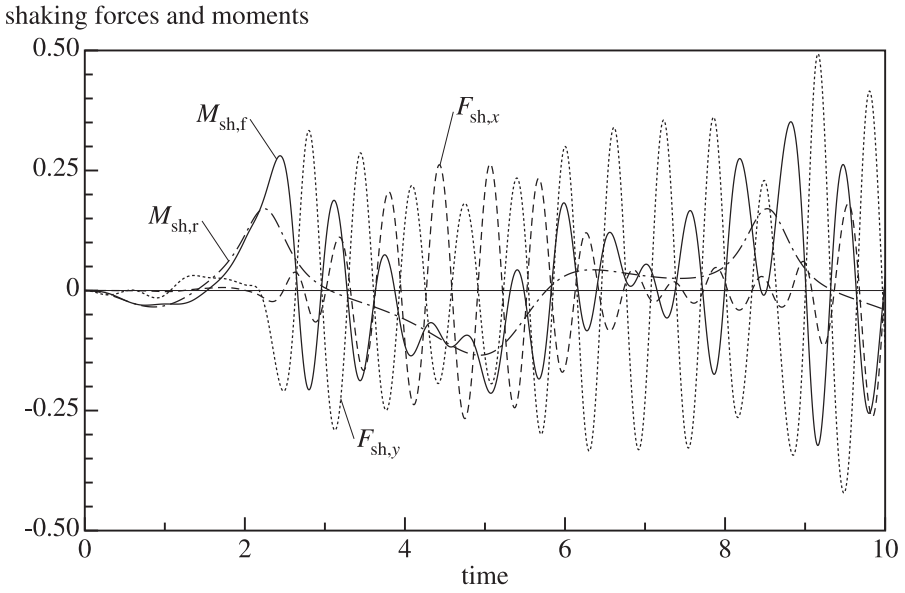

Fig. 10. Dimensionless shaking forces and shaking moments for the nominal case with hinges at the coupler ends: moment for the rigid case ($M_{sh,r}$, dash-dotted), moment for the flexible case ($M_{sh,f}$, continuous), force in the x-direction ($F_{sh,x}$, dashed) and force in the y-direction ($F_{sh,y}$, dotted).

balance for the rigid mechanism with $\xi_0 = \pm\sqrt{3}/6$ [2]. The crank is spun up from rest to a constant angular velocity according to the profile for its prescribed angle θ_1 of the form of Eq. (9). In the examples, the values $\Omega = 1$ and $T_1 = 2$ are chosen and the total length of the simulation interval is 10 with a total rotation angle of 9 rad.

If the same properties are chosen for the coupler as for the longer beam in the rotator of Section 2, the unit of length is 0.1 m, the unit of mass is 0.0024 kg and the unit of time is 0.02309 s. The corresponding units for force, moment and flexural rigidity are 0.45 N, 0.045 N m and 0.0045 N m^2, respectively. Results will be presented in a dimensionless form.

The beam model simulated in Spacar is the classical Euler–Bernoulli beam with neglected elongation and shear deformation, and the mass distribution is assumed to be a line mass, so no moments of inertia of the cross-section are taken into account. Typically, 16 beam elements are used to model the flexible coupler. This gives an error smaller than one percent for the frequencies of the first eight vibration modes.

As a reference case, a coupler hinged at its ends to the crank and the rocker is considered first. The resulting shaking moment with respect to the nominal centre of mass S for the case in which the coupler is rigid and the two components of the shaking force and the shaking moment for the flexible case are shown in Fig. 10. The main frequency contribution results from the first eigenmode with a frequency of $\pi/2$.

Next, the case in which the coupler is hinged at the two nodes of the first bending natural mode is considered. As the total length of the coupler is larger than in the reference case, its mass m_2 is larger and the frequency is lower: the first eigenfrequency is now 1.084. The resulting shaking forces and moments are shown in Fig. 11. The shaking forces are now free of the first bending mode frequency and the main component is in the third bending mode with a frequency of 3.486. The shaking moment shows the rigid-body motion and the second bending mode with a frequency of 2.028. The amplitude of the shaking forces is considerably reduced with respect to the reference case, by about a factor of 20. Also the shaking moments have been reduced, but not as much as the shaking forces, by about a factor of 2.

In the case the coupler is hinged at the reciprocal points on the radius of gyration, the results become as shown in Fig. 12. It should be noted that the mass of the coupler is smaller than in the previous case, but higher than in the reference case. The rigid-body part in the shaking moment has disappeared, as expected, and also the amplitude of the second bending mode with a frequency of 2.391 has been reduced, which is now a factor of 6 smaller than in the reference case. On the other hand, the amplitudes of the shaking forces have increased and both the fundamental bending frequency of 1.180 and the third bending mode with a frequency of 3.837 are clearly visible; the reduction with respect to the reference case is still about 12.

Finally, the case in which the first, third and fifth bending modes are force balanced is considered. In this case, the coupler is supported at four points given in Eq. (34) and the displacements at either side of the coupler are combined with a whippletree as shown in Fig. 13 to displacements at the hinges connected to the crank and the rocker, where the coupler is supported at the points C_1, C_2, C_3 and C_4; the hinge points at the crank, A_1, and the rocker, A_2, are at $\xi = \xi_0 = \pm 2(W_3\xi_3 + W_4\xi_4) = \pm 0.255872813$. The results are shown in Fig. 14, where the shaking forces have been scaled up by a factor of ten to make them visible in the same graph as the shaking moments. The main contribution now comes from the seventh bending mode with a frequency of 13.44. It is indeed seen that the shaking forces have become significantly small, as they are reduced by a factor of about 200 with respect to the reference case, but that the shaking moments have increased, although they are still a factor 2 smaller than in the reference

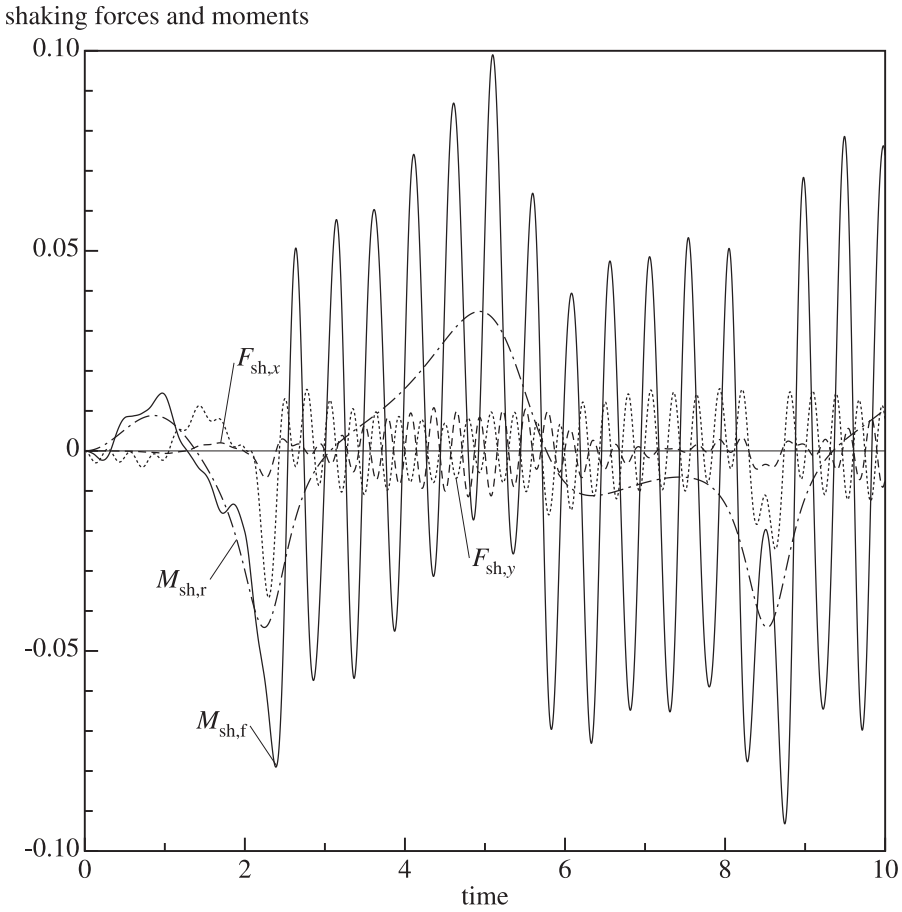

Fig. 11. Shaking forces and shaking moments for the case in which the coupler is hinged at the nodes of the first bending mode. The meaning of the lines is the same as in Fig. 10.

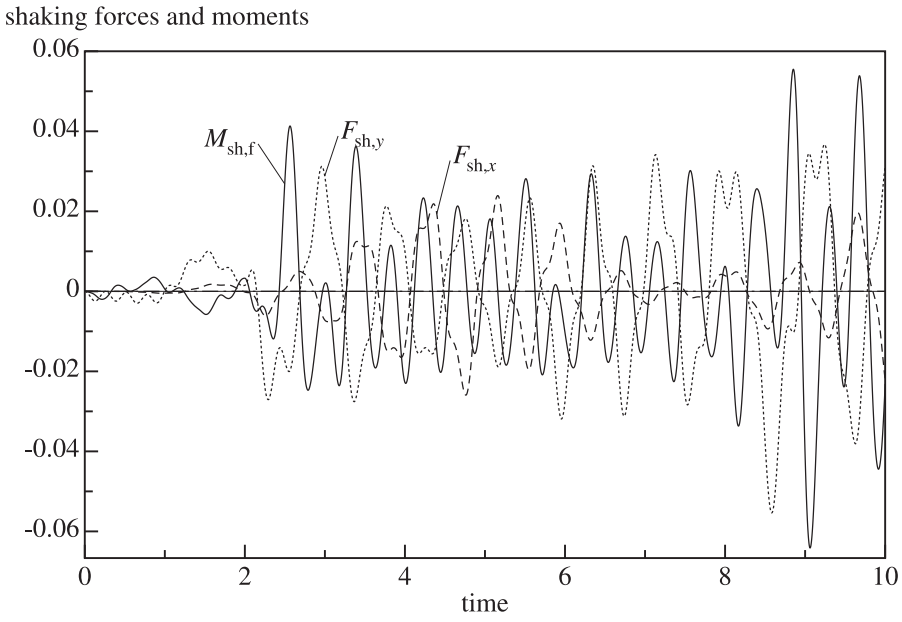

Fig. 12. Shaking forces and shaking moments for the case in which the coupler is hinged at the reciprocal points. The meaning of the lines is the same as in Fig. 10.

Fig. 13. Whippletree support of the coupler.

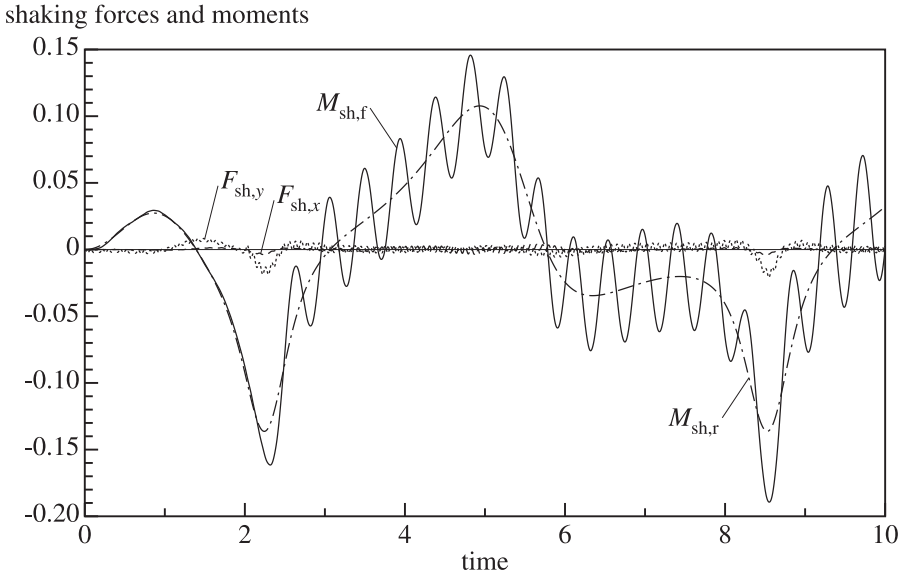

Fig. 14. Shaking forces and shaking moments for the case in which the coupler is hinged at four points as in Eq. (34). The shaking forces have been scaled up by a factor of ten. The meaning of the lines is the same as in Fig. 10.

case. This increase with respect to the examples of Figs. 11 and 12 is mainly due to the contribution of the rigid-body motion, as the value of ξ_0 is far off its ideal value of $\sqrt{3}/6$ and the mass m_2 is larger, but also a component with a frequency of 2.289 of the second bending mode is clearly visible.

6. Conclusions

Two approaches to the dynamic balance of mechanisms with flexible links have been introduced. One is based on similarity of a mechanism and a balancing mechanism, where the balancing mechanism is a scaled version of the mechanism with the same dynamic behaviour. The other is based on modal balancing, where the mechanism is designed in such a way that the lowest-order linear vibration modes give no shaking forces or shaking moments.

For a single rotator, the functional link and its balancing link have to be similar in shape and the speed of sound has to be proportional to their dimensions in order to obtain a perfect balance. As these conditions can be challenging in practice, approximations have to be made, which, nevertheless, lead to designs with a large reduction of the shaking forces.

Two rotators can be combined to obtain a balanced translator. As the balancing mechanism cannot be similar to the functional translator, unless it is identical, perfect balance is not possible, but still, a significant reduction of the shaking forces can be accomplished; in a representative example, the reduction was by more than a factor of 100 and for a symmetric forcing even by a factor of 1500.

The application to the dynamic balancing of the flexible coupler of a four-bar mechanism shows a reduction of shaking forces by factors from 20 for a coupler supported at two points up to 200 for a coupler supported at four points with a whippletree. The shaking moment is reduced by a factor of at least two with respect to the reference case. If the configuration with a full balance for the rigid-body case is chosen, a fairly good reduction of the shaking force by a factor of 12 and of the shaking moment by a factor of 6 is observed. Apparently, there is a trade-off between force balance and moment balance: a good dynamic force balance may lead to an increased shaking moment.

Although the methods are explained for and applied to planar mechanisms, they can, in principle, be equally applied to spatial mechanisms. Some freedom in the design is lost, as the similarity has to be maintained in all directions or vibration modes of links in two directions need to have nodes at the same positions.

A direction of future research is a further investigation of good compromises. Furthermore, cases of non-uniform beams and the inclusion of the mass of the joints and the auxiliary mechanisms need to be considered.

Declaration of competing interest

The authors declare that they have no known competing financial interests or personal relationships that could have appeared to influence the work reported in this paper.

References

[1] R.S. Berkof, G.G. Lowen, A new method for completely force balancing simple linkages, Trans. ASME, J. Eng. Ind. 91 (1969) 21–26.
[2] R.S. Berkof, Complete force and moment balancing of inline four-bar linkages, Mech. Mach. Theory 8 (1973) 397–410.
[3] V.H. Arakelian, M.R. Smith, Complete shaking force and shaking moment balancing of linkages, Mech. Mach. Theory 34 (1999) 1141–1153.
[4] S. Briot, I.A. Bonev, C.M. Gosselin, V. Arakelian, Complete shaking force and shaking moment balancing of planar parallel manipulators with prismatic pairs, Proc. Inst. Mech. Eng. K 223 (2009) 43–52.
[5] V. van der Wijk, Methodology for Analysis and Synthesis of Inherently Force and Moment-Balanced Mechanisms (Ph. D. thesis), Universiteit Twente, Enschede, 2014.
[6] K. Chaudhary, H. Chaudhary, Optimal dynamic balancing and shape synthesis of links in planar mechanisms, Mech. Mach. Theory 93 (2015) 127–146.
[7] G.G. Lowen, R.S. Berkof, Survey of investigations into the balancing of linkages, J. Mech. 3 (1968) 221–231.
[8] G.G. Lowen, F.R. Tepper, R.S. Berkof, Balancing of linkages - an update, Mech. Mach. Theory 18 (1983) 213–220.
[9] V.H. Arakelian, M.R. Smith, Shaking force and shaking moment balancing of mechanisms: a historical review with new examples, Trans. ASME, J. Mech. Des. 127 (2005) 334–339, erratum ibid. 1034–1035.
[10] B. Wei, D. Zhang, A review of dynamic balancing for robotic mechanisms, Robotica 39 (2021) 55–71.
[11] A. Meldahl, Auswuchten elastischer Rotoren, Z. Angew. Math. Mech. 34 (1954) 317–318.
[12] K. Federn, Grundlagen einer systematischen Schwingungsentstörung wellenelastischer Rotoren, in: Swingungsabwehr, Vorträge der VDI-Tagung Essen 1956, VDI-Verlag, VDI-Berichte 24, Düsseldorf, 1957, pp. 9–25.
[13] R.E.D. Bishop, G.M.L. Gladwell, The vibration and balancing of an unbalanced flexible rotor, J. Mech. Eng. Sci. 1 (1959) 66–77.
[14] S.H. Crandall, Rotordynamics, in: W. Kliemann, N. Sri Namachchivaya (Eds.), Nonlinear Dynamics and Stochastic Mechanics, CRC Press, Boca Raton, 1995, pp. 3–44.
[15] W.C. Foiles, P.E. Allaire, E.J. Gunter, Review: rotor balancing, Shock Vib. 5 (1998) 325–336.
[16] M.I. Friswell, J.E.T. Penny, S.D. Garvey, A.W. Lees, Dynamics of Rotating Machines, Cambridge University Press, New York, 2010.
[17] M.J. Walker, R.S. Haines, An experimental study of the effects of counterweights on a six-bar chain, Mech. Mach. Theory 17 (1982) 355–360.
[18] F. Xi, R. Sinatra, Effect of dynamic balancing on four-bar linkage vibrations, Mech. Mach. Theory 32 (1997) 715–728.
[19] Y.-Q. Yu, J. Lin, Active balancing of a flexible linkage with redundant drives, Trans. ASME, J. Mech. Des. 125 (2003) 119–123.
[20] Y.-Q. Yu, B. Jiang, Analytical and experimental study on the dynamic balancing of flexible mechanisms, Mech. Mach. Theory 42 (2007) 626–635.
[21] R. Cross, Center of percussion of hand-held implements, Amer. J. Phys. 72 (2004) 622–630.
[22] V.J. Kalas, Shaking Force Balance in Parallel Manipulators with Flexible Links (Master Thesis, report WA-1588), Laboratory of Mechanical Automation and Mechatronics, Faculty of Engineering Technology, University of Twente, Enschede, 2016.
[23] L.L. Howell, Compliant Mechanisms, Wiley, New York, 2001.
[24] J.B. Jonker, J.P. Meijaard, SPACAR - computer program for dynamic analysis of flexible spatial mechanisms and manipulators, in: W. Schiehlen (Ed.), Multibody Systems Handbook, Springer-Verlag, Heidelberg, 1990, pp. 123–143.
[25] S. Martínez, J.P. Meijaard, V. van der Wijk, On the shaking force balancing of compliant mechanisms, in: Proceedings of the 7th International Conference on Control, Mechatronics and Automation (ICCMA), IEEE, Piscataway NJ, 2019, pp. 310–314.
[26] J.P. Meijaard, V. van der Wijk, On the dynamic balance of a planar four-bar mechanism with a flexible coupler, in: T. Uhl (Ed.), Advances in Mechanism and Machine Science, Proceedings of the 15th IFToMM World Congress on Mechanism and Machine Science, Springer Nature Switzerland, Cham, 2019, pp. 3037–3046.
[27] J.P. Meijaard, Validation of flexible beam elements in dynamics programs, Nonlinear Dynam. 9 (1996) 21–36.
[28] J.P. den Hartog, Mechanical Vibrations, fourth ed., McGraw-Hill, New York, 1956.
[29] L.E. Nijdam, Dynamic Balance Principles Based on a Flexible Beam for the Synthesis of Dynamically Balanced Compliant Mechanisms (Master Thesis), Delft University of Technology, Delft, 2021.
[30] V. van der Wijk, J.L. Herder, B. Demeulenaere, Comparison of various dynamic balancing principles regarding additional mass and additional inertia, Trans. ASME, J. Mech. Robot. 1 (2009) 041006-1–041006-9.